Differential requirement of MALT1 for BAFF-induced outcomes in B cell subsets

Michael W. Tusche,[1,3] Lesley A. Ward,[1] Frances Vu,[1] Doug McCarthy,[1] Miguel Quintela-Fandino,[3] Jurgen Ruland,[4] Jennifer L. Gommerman,[1] and Tak W. Mak[1,2,3]

[1]Department of Immunology and [2]Department of Medical Biophysics, Faculty of Medicine, University of Toronto, Toronto, Ontario M5S 1A8, Canada
[3]Campbell Family Institute for Cancer Research, Princess Margaret Hospital, Toronto, Ontario M5G 2C1, Canada
[4]Technische Universität München, 81675 Munich, Germany

B cell activation factor of the TNF family (BAFF) activates noncanonical nuclear factor κB (NF-κB) heterodimers that promote B cell survival. We show that although MALT1 is largely dispensable for canonical NF-κB signaling downstream of the B cell receptor, the absence of MALT1 results in impaired BAFF-induced phosphorylation of NF-κB2 (p100), p100 degradation, and RelB nuclear translocation in B220$^+$ B cells. This corresponds with impaired survival of MALT1$^{-/-}$ marginal zone (MZ) but not follicular B cells in response to BAFF stimulation in vitro. MALT1$^{-/-}$ MZ B cells also express higher amounts of TRAF3, a known negative regulator of BAFF receptor–mediated signaling, and TRAF3 was found to interact with MALT1. Furthermore, phenotypes associated with overexpression of BAFF, including increased MZ B cell numbers, elevated serum immunoglobulin titers, and spontaneous germinal center formation, were found to be dependent on B cell–intrinsic MALT1 expression. Our results demonstrate a novel role for MALT1 in biological outcomes induced by BAFF-mediated signal transduction.

CORRESPONDENCE
Tak W. Mak:
tmak@uhnresearch.ca
OR
Jennifer L. Gommerman:
jen.gommerman@utoronto.ca

Abbreviations used: BAFF, B cell activation factor of the TNF family; BCMA, B cell maturation antigen; CGG, chicken γ-globulin; FO, follicular; GC, germinal center; IKK, IκB kinase; MZ, marginal zone; NIK, NF-κB–inducing kinase; PI, propidium iodide; PI3-kinase, phosphoinositide 3-kinase; TACI, transmembrane activator and calcium modulator and cyclophilin ligand interactor; Td, T dependent; Ti, T independent.

The NF-κB family of heterodimeric transcription factors plays a critical role in cellular functions such as immunoregulation, inflammation, cell survival, and cell-cycle progression (Li and Verma, 2002; Hayden and Ghosh, 2004). NF-κB subunits include RelA (p65), RelB, c-Rel, NF-κB1 (p50), and NF-κB2 (p52). NF-κB1 and NF-κB2 are synthesized as large precursors (p105 and p100, respectively) that are processed to the transcriptionally active p50 and p52 subunits in response to cytokine signaling.

NF-κB heterodimers are activated by either a canonical or a noncanonical pathway (Hayden and Ghosh, 2004). The canonical pathway depends on activation of IκB kinase (IKK) β, which phosphorylates inhibitory IκB molecules bound to NF-κB subunits such as RelA, allowing NF-κB to translocate to the nucleus (Hayden and Ghosh, 2004). The noncanonical pathway depends on activation of IKKα (Senftleben et al., 2001). NF-κB–inducing kinase (NIK) phosphorylates and activates IKKα in response to various stimuli (Ling et al., 1998). NIK has also been shown to phosphorylate p100 at serines 866 and 870 (Xiao et al., 2001). Activated IKKα then drives the serine phosphorylation of IκB-like domains within the NF-κB subunits themselves, such as those present in NF-κB2 p100 (Senftleben et al., 2001). Polyubiquitination and degradation of these phosphorylated domains allows p52 to enter the nucleus.

A known activator of noncanonical NF-κB signaling is B cell activation factor of the TNF family (BAFF; also known as BLyS, TALL-1, THANK, zTNF-1, and TNFSF13B; Schneider et al., 1999). In particular, BAFF induces the processing of p100 to p52 (Claudio et al., 2002; Kayagaki et al., 2002). BAFF is expressed by neutrophils, monocytes, and dendritic cells (Nardelli et al., 2001), and promotes B cell survival by up-regulating the antiapoptotic molecules Bcl-2 and Bcl-xL (Mackay et al., 1999; Batten et al., 2000; Schiemann et al., 2001). BAFF can also induce cell-cycle entry by triggering cyclin D2

J.L. Gommerman and T.W. Mak contributed equally to this paper.

The Rockefeller University Press $30.00
J. Exp. Med. Vol. 206 No. 12 2671-2683
www.jem.org/cgi/doi/10.1084/jem.20091802

synthesis (Huang et al., 2004). BAFF-induced transitional B cell survival is required for the development of mature B cell subsets, including $CD21^{low}CD23^{high}$ follicular (FO) B cells as well as $CD21^{high}CD23^{low}$ marginal zone (MZ) B cells (Batten et al., 2000). Mice that overexpress BAFF (BAFF-Tg) exhibit an expanded MZ B cell compartment, hyper-Ig production, and spontaneous germinal center (GC) formation concomitant with autoimmune symptoms (Mackay et al., 1999; Khare et al., 2000).

BAFF binds to three different receptors: B cell maturation antigen (BCMA; Marsters et al., 2000; Thompson et al., 2000), transmembrane activator and calcium modulator and cyclophilin ligand interactor (TACI; Marsters et al., 2000; Thompson et al., 2000; Wu et al., 2000), and BAFF-R (Thompson et al., 2001; Yan et al., 2001). Knockout studies have shown that the functions of these receptors are distinct, with only BAFF-R being necessary for B cell survival and maturation (Sasaki et al., 2004). Signals downstream of the BAFF-R are known to activate noncanonical NF-κB heterodimers (Claudio et al., 2002; Kayagaki et al., 2002), and $BAFF^{-/-}$ mice exhibit a complete block in FO and MZ B cell development (Schiemann et al., 2001). However, mice with deficiencies or harboring mutations for various elements of the NF-κB2 pathway used by BAFF-R signaling, such as RelB and NIK (Shinkura et al., 1999; Weih et al., 2001), do not completely phenocopy $BAFF^{-/-}$ mice in terms of B cell development. This suggests that various parallel pathways emanate from the BAFF-R that leads to the development of different B cell subsets.

MALT1 and Bcl10 are signal integrators that are crucial for canonical NF-κB activation downstream of the TCR (Ruland et al., 2001, 2003; Ruefli-Brasse et al., 2003; Xue et al., 2003). However, the role of MALT1 downstream of the BCR is more subtle and not essential for the manifestation of many BCR-derived signals (Ruefli-Brasse et al., 2003; Ruland et al., 2003). Because $MALT1^{-/-}$ mice exhibit a reduction in MZ and B1 B cells, this raises the question that perhaps MALT1 may be involved in BAFF-R–mediated signaling to maintain some but not all B cell subsets. In this study, we show that MALT1 is necessary for BAFF-induced survival of MZ B cells but not FO B cells, and is involved in the optimal activation of NF-κB2 in B cells stimulated with BAFF. In addition, the phenotype of BAFF-Tg mice is dependent on MALT1 in spite of the fact that MALT1 is not essential for BCR signaling in vitro.

RESULTS

MALT1 is not essential for B cell proliferation, B cell survival, IκBα degradation, and NF-κB activation induced by BCR engagement

Several groups have shown that MALT1 is necessary for MZ and B1 B cell development, whereas Bcl10 leads to a more profound developmental defect affecting FO, MZ, and B1 B cells (Ruefli-Brasse et al., 2003; Ruland et al., 2003; Xue et al., 2003). Though Bcl10 has been shown to impinge on the activation of NF-κB downstream of both TCR and BCR and is essential for B cell survival, MALT1 appears to play a more subtle role in B cell survival after BCR engagement, and its role in the survival of FO versus MZ B cells has not been determined (Ruefli-Brasse et al., 2003; Ruland et al., 2003). We first examined whether MALT1 is required for B cell proliferation triggered by BCR engagement by stimulating purified, resting $B220^+$ B cells from WT, $MALT1^{-/-}$, and $Bcl10^{-/-}$ mice with anti-IgM and monitoring [^{3}H]thymidine incorporation. As expected, the proliferation of $Bcl10^{-/-}$ B cells was significantly reduced, but no statistically significant difference in proliferation was noted between WT and $MALT1^{-/-}$ B cells (Fig. 1 A, i). $MALT1^{+/+}$ and $MALT1^{-/-}$ B cells were also treated with increasing doses of anti-IgM, and proliferation was assessed at 24 h (Fig. 1 A, ii). No significant differences were noted between genotypes. Consistent with this result, anti-IgM treatment stimulated IκBα degradation in WT and $MALT1^{-/-}$ B cells but not in $Bcl10^{-/-}$ B cells (Fig. 1 B). Furthermore, anti-IgM induced the up-regulation of p65-dependent DNA binding in WT and $MALT1^{-/-}$ B cells but not in $Bcl10^{-/-}$ B cells (Fig. 1 C). The CD40 pathway is also important in B cell activation and proliferation. We therefore also examined the role of MALT1 in anti-CD40–mediated B cell proliferation. We found no differences in B cell proliferation in response to anti-CD40 treatment of WT versus $MALT1^{-/-}$ B cells (Fig. 1 A, iii). Furthermore, CD40L stimulation also induced IκBα degradation and p100 processing in WT and $MALT1^{-/-}$ B cells (Fig. S1, A and B). Therefore, our data imply that CD40-mediated signaling pathways are intact in $MALT1^{-/-}$ B cells.

A subtle role for MALT1 in B cell survival has been previously demonstrated (Ferch et al., 2007), but B cell survival and activation of $MALT1^{-/-}$ MZ versus FO B cells has not been examined. We therefore sorted, FO and the small number of MZ B cells from $MALT1^{-/-}$ and WT mice (Fig. S2) and evaluated different parameters after BCR stimulation. In agreement with another report (Ferch et al., 2007), $MALT1^{-/-}$ FO B cells were slightly more susceptible to IgM-induced cell death. However $MALT1^{-/-}$ MZ B cells responded much like $MALT1^{+/+}$ MZ B cells (Fig. 1 D). Because MZ B cells are prone to die in culture in response to anti-BCR stimulation, we examined the up-regulation of B7-2 on MZ B cells that is linked to BCR simulation (Oliver et al., 1997). We found that B7.2 was equally up-regulated in $MALT1^{+/+}$ and $MALT1^{-/-}$ MZ B cells, and FO B cells treated with anti-IgM stimulation (Fig. 1 E). In addition, sorted T2 cells from $MALT1^{+/+}$ and $MALT1^{-/-}$ mice were found to have similar survival responses (Fig. S3 A) and B7.2 up-regulation profiles in response to anti-BCR stimulation (Fig. S3 B). Collectively, MALT1 is not essential for IgM-induced IκBα degradation or p65 DNA binding nor is it absolutely required for the survival of FO, MZ, and T2 B cells, or for anti-BCR–induced B7-2 up-regulation in these B cells subsets.

BAFF-induced p100 phosphorylation and degradation are diminished in $MALT1^{-/-}$ B cells

Given that $MALT1^{-/-}$ mice exhibit a reduction in MZ and B1 B cells and that BCR signaling in $MALT1^{-/-}$ B cells is

largely intact, we hypothesized that MALT1 may be important for BAFF-dependent B cell survival signals for the maintenance of some B cell subsets. To evaluate the role of MALT1 in noncanonical NF-κB signaling, we stimulated purified WT and MALT1$^{-/-}$ resting B cells with recombinant BAFF and examined NF-κB2 (p100) degradation. We first confirmed that MALT1$^{-/-}$ splenic B cells expressed WT levels of BAFF-R (Fig. S4), as well as normal levels of signaling intermediates downstream of BAFF-R such as RelB, p100, and TRAF2 (Fig. 2 A and not depicted). Immunoblotting showed that in BAFF-stimulated WT B220^{+} B cells, p100 was degraded to yield the transcriptionally active p52 subunit (Fig. 2 A, cytoplasmic), concomitant with an increase in nuclear p52 (Fig. 2 A, nuclear). In contrast, MALT1$^{-/-}$ B cells generated reduced levels of p52 in response to BAFF (Fig. 2 A, cytoplasmic). BAFF stimulation also led to the nuclear accumulation of RelB in WT B cells, which was reduced in MALT1$^{-/-}$ B cells (Fig. 2 A, nuclear). Therefore, BAFF-dependent activation of NF-κB2 is impaired in MALT1$^{-/-}$ B cells.

Certain B cell populations are known to be underrepresented in MALT1$^{-/-}$ mice, particularly CD21^{high}CD23^{low}

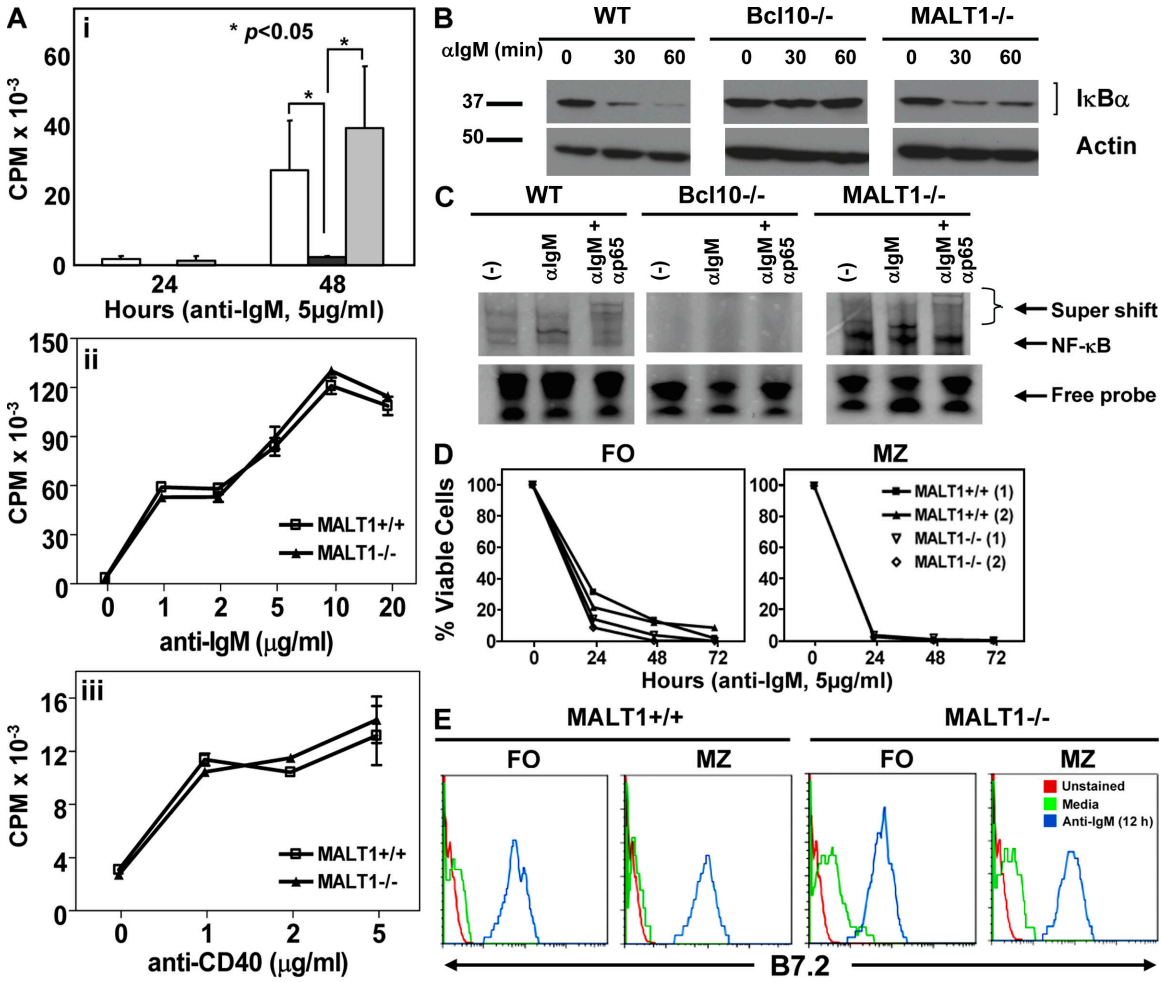

Figure 1. MALT1 is dispensable for B cell proliferation and canonical NF-κB activation induced by BCR engagement. (A) B220^{+} B cells were isolated from spleens of WT (white bars), Bcl10$^{-/-}$ (black bars), and MALT1$^{-/-}$ (gray bars) mice and stimulated for 24 or 48 h with 5 μg/ml anti-IgM (i), or for 24 h with the indicated doses of anti-IgM (ii) or anti-CD40 (iii). Proliferation was assessed by [^{3}H]thymidine incorporation. Results shown are means ± SD of three replicates per genotype and are representative of three independent analyses. (B) Purified splenic B cells from WT, Bcl10$^{-/-}$, and MALT1$^{-/-}$ mice were stimulated with 5 μg/ml anti-IgM for the indicated times, and lysates were Western blotted to detect IκBα. Results shown are representative of three independent analyses. (C) Nuclear lysates were prepared from unstimulated B cells or from B cells that had been treated for 8 h with anti-IgM from the indicated genotypes. Lysates were subjected to EMSA to detect up-regulation of binding to NF-κB DNA consensus sequences (p65). Results shown are representative of at least three independent analyses. (D) MZ and FO B cells were sorted from the indicated genotypes. Cells were treated with 5 μg/ml anti-IgM for the indicated times, and viability was assessed using annexin V/PI staining as described. Experiments shown are representative of three independent analyses. (E) Splenocytes from the indicated genotypes were cultured for 12 h with 5 μg/ml anti-IgM, and B7 up-regulation was assessed in the MZ and FO compartments as described in Materials and methods. Anti-IgM–treated samples (blue) were treated with 5 μg/ml for 12 h. Numbers to the left of gels represent kilodaltons.

MZ B cells. To exclude the possibility that the p100 degradation defect was merely caused by an absence of certain BAFF-responsive B cell subsets, we used phospho-flow cytometry to assess p100 phosphorylation in unfractionated as well as sorted MZ versus FO B cell populations. Although rare, we were able to sort sufficient numbers of $CD23^{low}$ B cells from $MALT1^{-/-}$ mice, and these were confirmed not to be T1 B cells because of high expression of CD21 (Fig. S2). After a 15-min treatment with recombinant BAFF, WT B cells exhibited a shift in phospho-p100 (serines 866 and 870) compared with unstimulated controls that was evident in total unfractionated B cells ($B220^{+}$), FO B cells ($CD23^{high}CD21^{low}$), and MZ B cells ($CD23^{low}CD21^{high}$; Fig. 2 B). Phospho-p100 returned to baseline levels after 60 min of treatment. In contrast, BAFF-induced p100 phosphorylation was not observed in total $MALT1^{-/-}$ B cells or in the fractionated MZ or FO B cell subsets (Fig. 2 B). Thus, MALT1 is involved in BAFF-induced p100 phosphorylation and degradation in both MZ and FO B cell compartments.

To further elucidate the role of MALT1 in BAFF signal transduction, we ablated MALT1 expression using RNAi-mediated silencing. Using BJAB cells that express BAFF-R but not BCMA or TACI (Thompson et al., 2001), we observed a nearly complete silencing of MALT1 expression (Fig. 2 C, cytoplasmic). Nuclear translocation of RelB induced by BAFF was found to be impaired in BJAB MALT1 knockdown cells compared with cells nucleofected with scrambled siRNA control (Fig. 2 C, nuclear). BJAB cells appear to have a high level of basal p100 processing (unpublished data), making it difficult to observe differences in p100 degradation in the absence of MALT1 in this particular cell line. Nevertheless, increases in phospho-p100 induced by BAFF pretreatment were absent in MALT1 knockdown BJAB cells compared with controls (Fig. 2 D). To validate the p100 phosphorylation readout, we also performed a knockdown of p100 in BJAB cells (Fig. 2 D, right) and found that staining for phospho-p100 was completely abolished in BJAB cells (Fig. 2 D, left). In addition, a p100 phospho-shift was not observed in

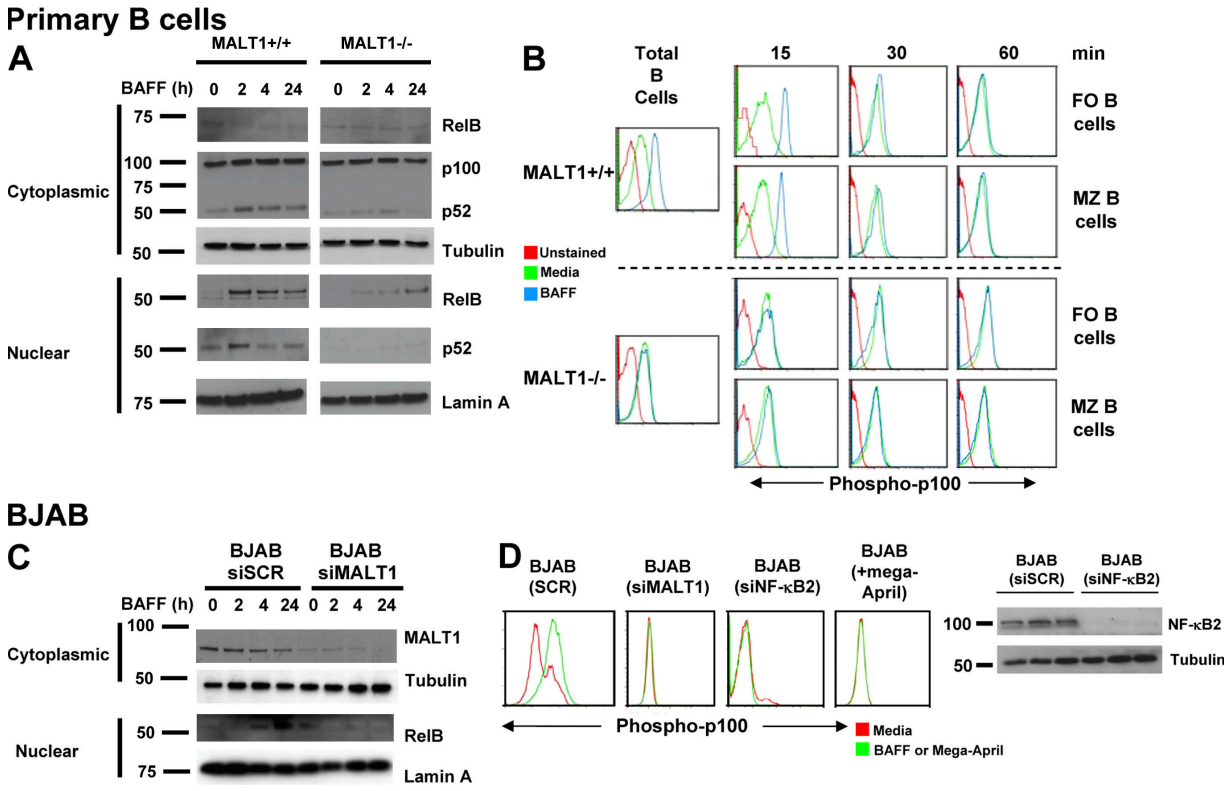

Figure 2. BAFF-induced p100 phosphorylation and degradation are diminished in $MALT1^{-/-}$ B cells. (A) Highly purified $B220^{+}$ cells from spleens of WT and $MALT1^{-/-}$ mice were stimulated with 2 µg/ml BAFF for the indicated times. Cytoplasmic lysates were Western blotted to detect p100, p52, RelB, and tubulin, and nuclear lysates were probed with anti-p52, anti-RelB, and lamin A as a loading control. Results shown are representative of four independent analyses. (B) BAFF-stimulated B cells were immunostained with anti-CD21–PE and anti-CD23–FITC, fixed, permeabilized, and stained for anti–phospho-p100. Results shown are representative of five independent analyses (n = 5 mice/genotype). (C) MALT1 was ablated in the BJAB cell line using nucleofected siRNA as described. Cells were collected 48 h after nucleofection, stimulated with BAFF, and lysed. Cytoplasmic lysates were probed with MALT1, and nuclear lysates were probed with RelB and lamin as described. Blots are representative of two independent analyses. (D) MALT1 was knocked down in BJAB cells, and intracellular phospho-flow detecting phosphorylation of p100 in response to BAFF or MegaAPRIL was conducted. Results are representative of three independent analyses. BJAB cells were also nucleofected with NF-κB2 siRNA and assessed for intracellular levels of phospho-p100. Protein levels in NF-κB2 knockdown BJAB cells compared with scrambled siRNA controls are also displayed. Results are representative of two independent analyses. Numbers to the left of gels represent kilodaltons.

BJAB cells treated with MegaAPRIL, a TACI/BCMA dual agonist, further indicating that the p100 phosphorylation in BJAB cells is exclusively mediated by BAFF-R rather than TACI and BCMA (Fig. 2 D). Collectively, these data confirm that MALT1 is necessary for an NF-κB2 signaling pathway triggered by stimulation of BAFF-R.

BAFF-induced survival and antiapoptotic gene induction are reduced in MALT1$^{-/-}$ CD21^{high}CD23^{low} MZ B cells

BAFF promotes B cell survival by activating the transcription of various antiapoptotic genes. To assess the role of MALT1 in BAFF-mediated survival, we treated purified, resting B220^{+} B cells with recombinant BAFF and assessed their viability by annexin V/propidium iodide (PI) staining over a time course. In preliminary experiments, no differences were observed between MALT1$^{+/+}$ and MALT1$^{-/-}$ B cells, depicted by the fold increase in viable cells (Fig. S4 A, left) or the percentage of viable cells (Fig. S4 A, right) after 48 h of culture. However, after 72 h of culture, WT B cells exhibited an ∼7.5-fold increase in survival over nonstimulated controls, whereas MALT1$^{-/-}$ B cells showed only a 3-fold increase in survival (Fig. S4 A, left). Unstimulated B cells isolated from WT or MALT1$^{-/-}$ mice showed no difference in survival (Fig. S4 A, right). Because BAFF does not expand FO B cells during protracted (72 h) in vitro culture (Batten et al., 2000), we postulated that the differences we observed at this time point were caused by preferential effects of BAFF on specific subsets of B cells. Therefore, we evaluated the viability of isolated FO versus MZ B cells from WT and MALT1$^{-/-}$ mice after 72 h of culture. Interestingly, we found that MALT1 was dispensable for BAFF-induced survival of BAFF-stimulated FO B cells (Fig. 3 A, i) but is necessary for optimal BAFF-stimulated MZ B cell survival (Fig. 3 A, ii). In addition, BAFF treatment up-regulated mRNAs for Bcl-2, Bcl-xL, cyclin D1, and cyclin D2 in FACS-sorted FO and MZ B cells from WT mice. Oligos used in real-time PCR analysis are displayed

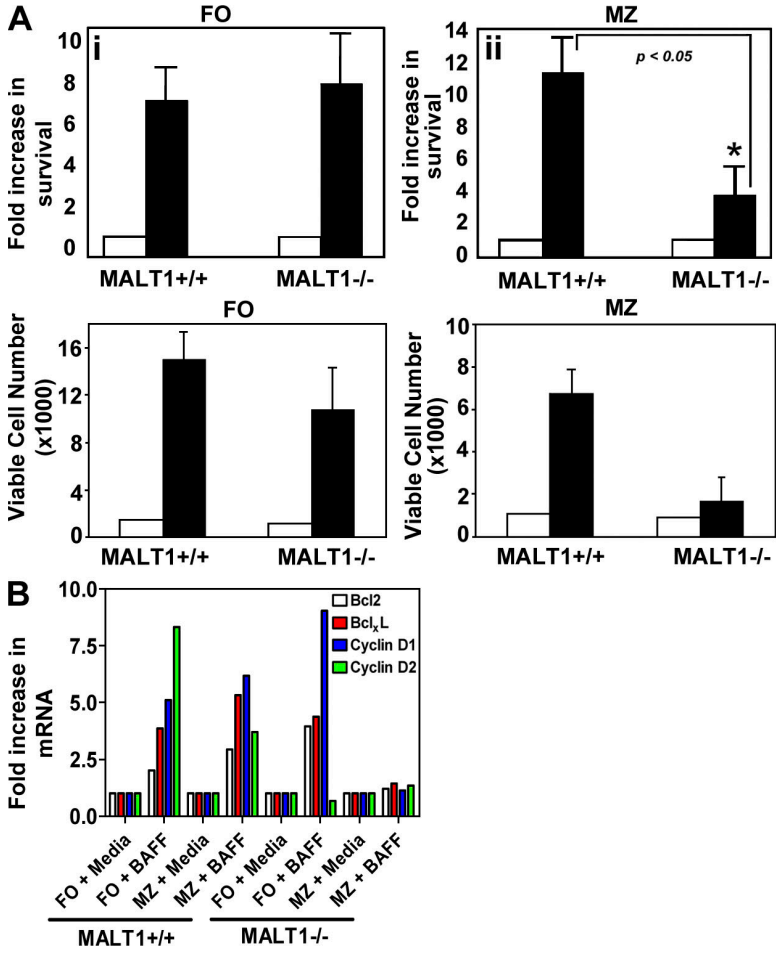

Figure 3. BAFF-induced survival and antiapoptotic gene induction are reduced in MALT1$^{-/-}$ B cells. (A) Fold increase in survival and absolute viable cell numbers of FO B cells (i) or MZ B cells (ii) isolated from the indicated genotypes and stimulated with BAFF for 72 h. Results shown are mean viabilities ± SD of four independent analyses with at least five mice per genotype. Black bars are BAFF treated and white bars are media controls. (B) cDNAs from unstimulated or BAFF-stimulated (2 µg/ml for 72 h) FO and MZ B cells from MALT1$^{+/+}$ and MALT1$^{-/-}$ mice were amplified using PCR to detect the indicated prosurvival factors. Results shown are mean fold increases in mRNA induction over unstimulated controls and are representative of three independent analyses.

in Table S2. However, 48 h of BAFF treatment failed to induce these prosurvival factors in MALT1$^{-/-}$ MZ B cells, whereas the fold induction of Bcl-2 and Bcl-xL and cyclin D1 in MALT1$^{-/-}$ FO B cells was similar to MALT1$^{+/+}$ controls (Fig. 3 B). Basal levels of the factors analyzed were found to be similar between WT and knockout in all cell types analyzed (unpublished data). Thus, MALT1 is important for BAFF-induced survival and for the up-regulation of antiapoptotic genes specifically in MZ B cells.

MALT1 interacts with TRAF3 and this interaction is negatively regulated by BAFF

TRAF3 has been shown to negatively regulate survival signals emanating from the BAFF-R, particularly in MZ B cells (Gardam et al., 2008). Because we have shown that MALT1 seems to preferentially regulate BAFF-mediated survival in the MZ compartment, we addressed whether TRAF3 levels were dysregulated in MALT$^{-/-}$ MZ B cells. Accordingly, cell lysates from sorted FO and MZ B cells were probed by Western blotting. TRAF3 was present at low levels in FO B cells, and no differences were observed between WT and MALT1$^{-/-}$ FO B cells (Fig. 4 A, left). However, MALT1$^{-/-}$ MZ B cells exhibited a baseline higher level of TRAF3 protein compared with MALT1$^{+/+}$ MZ B cells (Fig. 4 A, right). We next sought to determine whether MALT1 and TRAF3 form a complex that can be regulated by BAFF by stimulating BJAB cells with BAFF for 0, 2, 4, and 24 h, immunoprecipitated MALT1, and probed for TRAF3. In unstimulated cells, TRAF3 was found to form a complex with MALT1 that dissociated at 2 and 4 h, reforming at 24 h (Fig. 4 B). We also observed an association between MALT1 and TRAF3 in primary B220^{+} B cells that was relieved by treatment with BAFF (Fig. 4 C), although with slower kinetics. Therefore, TRAF3 levels are increased in the absence of MALT1, and TRAF3 forms a complex with MALT1 that is negatively regulated by BAFF stimulation.

BAFF-induced increases in serum Ig, MZ B cells, and B1 B cells are impaired in MALT1$^{-/-}$ mice

To examine the role of MALT1 in BAFF-dependent effects in vivo, we crossed MALT1$^{-/-}$ mice with BAFF-Tg mice. BAFF-Tg mice exhibit increases in some serum Ig isotypes. Therefore, we first conducted sandwich ELISAs on serum samples obtained from WT, BAFF-Tg, MALT1$^{-/-}$, and MALT1$^{-/-}$ × BAFF-Tg animals to assess if this was a MALT1-dependent phenomenon. Bcl10$^{-/-}$ and Bcl10$^{-/-}$ × BAFF-Tg mice, which were expected to be refractory to nonlimiting levels of BAFF because of the critical role of Bcl10 downstream of the BCR (Ruland et al., 2001; Xue et al., 2003), were analyzed in parallel as negative controls. The serum of BAFF-Tg mice contained significant increases in IgA, IgM, IgG_{2c}, and IgG_3 compared with nontransgenic WT controls (Fig. 5 A). More moderate increases in IgG_1 and IgG_{2b} were also observed in these animals. Sera from MALT1$^{-/-}$ and Bcl10$^{-/-}$ mice exhibited a marked reduction in all Ig isotypes analyzed, consistent with published reports (Ruland et al., 2001, 2003; Ruefli-Brasse et al., 2003; Xue et al., 2003). Strikingly, deficiency of either MALT1 or Bcl10 in the BAFF-Tg background led to significant decreases in all isotypes compared with BAFF-Tg controls (Fig. 5 A). We observed the same phenomenon when MALT1 was deficient only in B cells in BAFF-Tg mice (Fig. S6 A). Thus, the enhanced Ig production observed in BAFF-Tg mice requires not only Bcl10 but also B cell–intrinsic MALT1, and excess BAFF cannot restore the defective Ig production observed in Bcl10$^{-/-}$ and MALT1$^{-/-}$ mice.

B1 B cells are greatly reduced in Bcl10$^{-/-}$ and MALT1$^{-/-}$ mice (Ruland et al., 2001, 2003), and our flow cytometric analysis revealed that Bcl10$^{-/-}$ mice harbor an unusual population of CD5^{low}IgM^{low} cells in the peritoneal cavity (Fig. 5 B, top). We asked whether excess BAFF could rescue B1 B cells in the peritoneal cavity of Bcl10$^{-/-}$ and MALT1$^{-/-}$ mice. Bcl10 or MALT1 deficiency in a BAFF-Tg background resulted in frequencies of B1 B cells that were similar to Bcl10$^{-/-}$ and MALT1$^{-/-}$ mice (Fig. 5 B, top; and Fig. 5 C, left) The same was true when absolute numbers of B1 B cells were tabulated (Table S1). Therefore, excess BAFF cannot restore B1 B cells in Bcl10$^{-/-}$ and MALT1$^{-/-}$ mice.

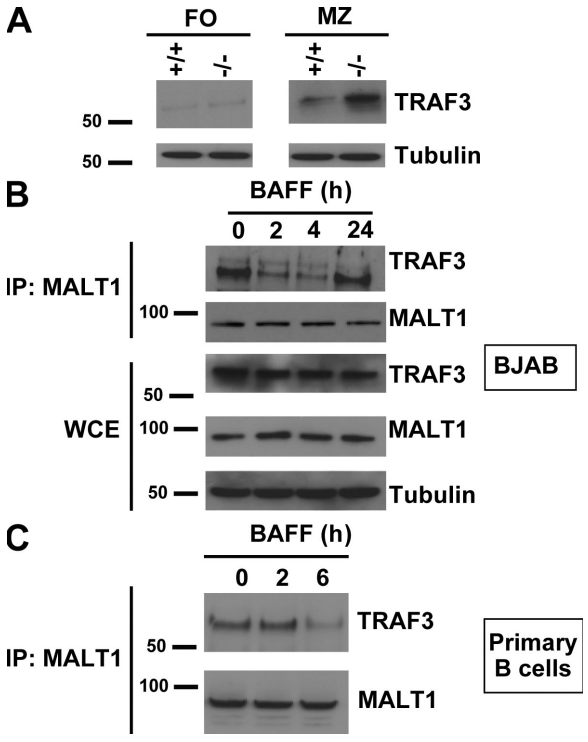

Figure 4. TRAF3 protein is increased in MALT1$^{-/-}$ MZ B cells, and MALT1 interacts with TRAF3 in a manner that is negatively regulated by BAFF. (A) MZ and FO B cells were isolated from the indicated genotypes. Lysates were obtained and Western blotted for TRAF3 and actin as a loading control. Blots are representative of four independent analyses. (B) BJAB cells or (C) primary B220^{+} B cells were starved for 2 h and stimulated with 2 µg/ml BAFF for the indicated times, and MALT1 was immunoprecipitated. Immunoprecipitates were probed with TRAF3 and MALT1 as a control. Whole cell extracts were probed with TRAF3, MALT1, and tubulin as a loading control. Numbers to the left of gels represent kilodaltons. IP, immunoprecipitation; WCE, whole cell extracts.

Although a lack of MALT1 did not alter total $B220^+CD23^+$ B cell numbers in the spleen (Table S1), flow cytometric analysis revealed altered homeostasis of MZ B cells. Because BAFF-Tg mice have a greatly expanded MZ B cell compartment (Fig. 5 B, bottom; and Fig. 5 C, right; Mackay et al., 1999) as well as a sixfold increase in the absolute numbers of these cells (Table S1), we asked if overexpression of BAFF could rescue MZ B cells in $MALT1^{-/-}$ mice. $Bcl10^{-/-}$ × BAFF-Tg and $MALT1^{-/-}$ × BAFF-Tg animals showed both a lower percentage (Fig. 5 B, bottom; and Fig. 5 C, right) and decreased absolute numbers (Table S1) of splenic MZ B cells compared with BAFF-Tg mice. A mild nonstatistically significant increase in MZ B cells was observed in the $MALT1^{-/-}$ × BAFF-Tg mice compared with the $MALT1^{-/-}$ mice, but this was significantly less than what was observed in the $MALT1^{+/+}$ × BAFF-Tg mice. In addition, a marked absence of $CD23^{low}CD21^{high}CD1d^{high}$ B cells was apparent in both of the $Bcl10^{-/-}$ backgrounds with or without the BAFF transgene (Fig. 5 B, bottom; and Fig. 5 C, right). Curiously, $Bcl10^{-/-}$ but not $MALT1^{-/-}$ mice exhibited an unusual population of $CD23^{low}CD21^{low}$ cells (with or without the BAFF transgene; Fig. 5 B, bottom). Collectively, our data confirm a significant reduction of MZ and B1 B cells in $MALT1^{-/-}$ and $Bcl10^{-/-}$ mice (Ruland et al., 2001, 2003; Ruefli-Brasse et al., 2003; Xue et al., 2003). Furthermore, these data demonstrate that the increases in MZ and B1 B cells caused by BAFF overexpression is dependent on MALT1 for their full manifestation. These results further corroborate our findings (Figs. 2–4) that BAFF-R–mediated activation of alternative NF-κB is impaired in the absence of MALT1.

Impaired T-dependent (Td) and T-independent (Ti) humoral responses in the absence of MALT1

BAFF-R is required for optimal Td B cell responses, and Ti responses are augmented in BAFF-Tg mice (Schneider, 2005). To assess whether MALT1 is important for the effects of BAFF on Td responses, we immunized WT, $MALT1^{-/-}$, and $Bcl10^{-/-}$ mice and their BAFF-Tg counterparts with the Td antigen NP–chicken γ-globulin (CGG). NP-CGG immunization induced a modest increase in the frequency of GC B cells (Fas^+GL7^+) in WT mice (Fig. 6, A and B). Numbers of GC B cells were already elevated in unimmunized BAFF-Tg mice, with a further increase observed when these mice were immunized (Fig. 6, A and B). However, even in the presence of excess BAFF antigen–specific B cell responses could not be mounted in the absence of MALT1, as judged by the frequency

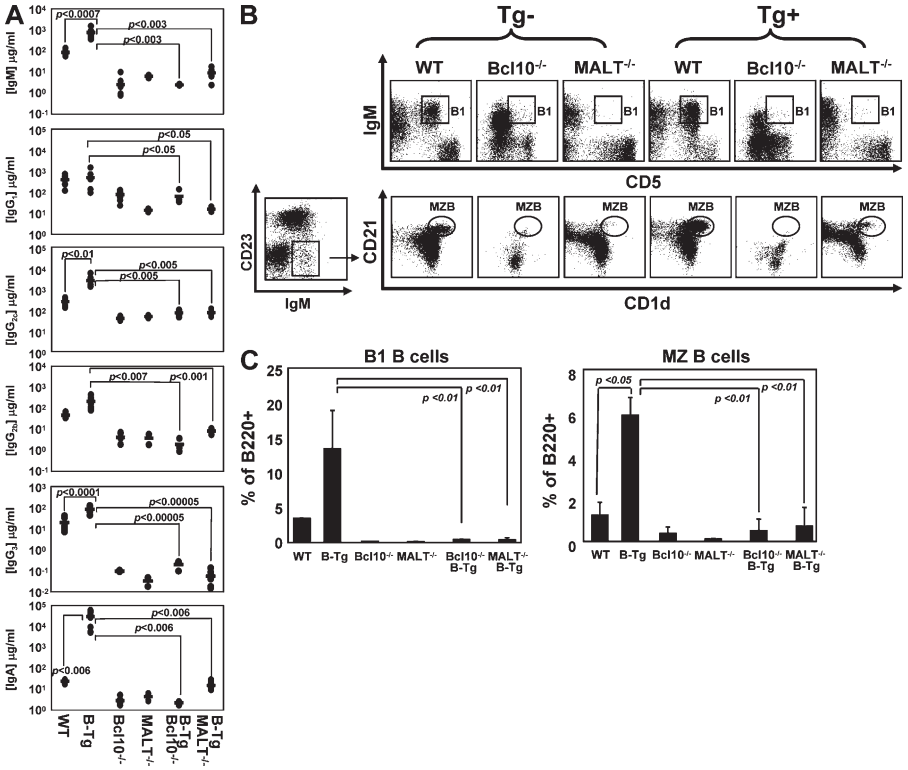

Figure 5. MALT1 is required for BAFF-induced increases in basal serum Ig, MZ B cells, and B1 B cells. (A) Serum samples from 8–10-wk-old mice of the indicated genotypes were analyzed by ELISA to detect the indicated Ig isotypes. Data shown are levels for individual mice (n = 3–9 mice/genotype) and the horizontal bars are means. Results shown are one trial representative of four independent analyses. (B) Peritoneal cells from 8–10-wk-old mice of the indicated genotypes were pregated on B220, and the B1 B cell population was isolated as $IgM^{high}CD5^{high}$ (top). Splenocytes from 8–10-wk-old mice of the indicated genotypes were pregated on B220 and CD23 (bottom). The $B220^{high}CD23^{low}$ population was isolated and further fractionated to examine MZ B cells ($CD21^{high}CD1d^{high}$). FACS plots shown are representative of six independent analyses. (C) The cells in B were quantified, and the results are expressed as mean percentages of $B220^+$ cells ± SD of four independent analyses (n = 6–14 mice/genotype). B-Tg, BAFF-Tg.

and numbers of total GC B cells (Fig. 6, A and B) and by measuring titers of low affinity (NP-30) and high affinity (NP-3) antibodies directed against NP-CGG (Fig. 6 C, left, top and bottom) or Ti antigen NP-Ficoll (Fig. 6 D). The same was true if MALT1 was absent exclusively in B cells in BAFF-Tg mice (Fig. S7). As expected, Bcl10$^{-/-}$ × BAFF-Tg mice also failed to mount a Td response in the presence or absence of the BAFF transgene (Fig. 6, A and B). Therefore, we observed that B cell–intrinsic expression of MALT1 is necessary to mount both Td and Ti response even in the presence of excess BAFF.

BAFF-induced GC formation in the spleen and Ig deposition in the kidney require MALT1

BAFF-Tg mice exhibit a high frequency of PNA^{+} GC networks in the absence of immunization (Mackay et al., 1999), a phenomenon we also observed (Fig. 7 A, top). In contrast, no PNA^{+} cells were identified in sections of spleens from MALT1$^{-/-}$ × BAFF-Tg animals, indicating that the formation of BAFF-induced spontaneous GCs requires MALT1. Similar results were obtained for Bcl10$^{-/-}$ × BAFF-Tg mice. In addition, BAFF-Tg spleens (from either the WT or mixed bone marrow chimeric backgrounds) that were stained with MAdCAM-1 to delineate the MZ sinus showed that the MZ was increased in size (Fig. 7 A, bottom). This MZ expansion was not observed in MALT1$^{-/-}$ × BAFF-Tg or Bcl10$^{-/-}$ × BAFF-Tg mice. Similar results were obtained for MALT1$^{-/-}$ and Bcl10$^{-/-}$ mixed bone marrow chimeras, suggesting a B cell–intrinsic requirement for MALT1/Bcl10 for an expanded MZ (Fig. S6 B).

BAFF-Tg mice exhibit mild glomerulonephritis characterized by Ig deposition in the kidney mesangium (McCarthy et al., 2006). Using immunofluorescence, we detected deposits of IgM, IgG, and IgA in sections of kidneys from BAFF-Tg animals (Fig. 7 B). These Ig deposits were not present in kidney sections obtained from MALT1$^{-/-}$ × BAFF-Tg or Bcl10$^{-/-}$ × BAFF-Tg mice (Fig. 7 B), or in mice where MALT1/Bcl10 are exclusively lacking in B cells (Fig. S6 B). Thus, the major histological abnormalities associated with BAFF overexpression require B cell–intrinsic MALT1 expression for their manifestation.

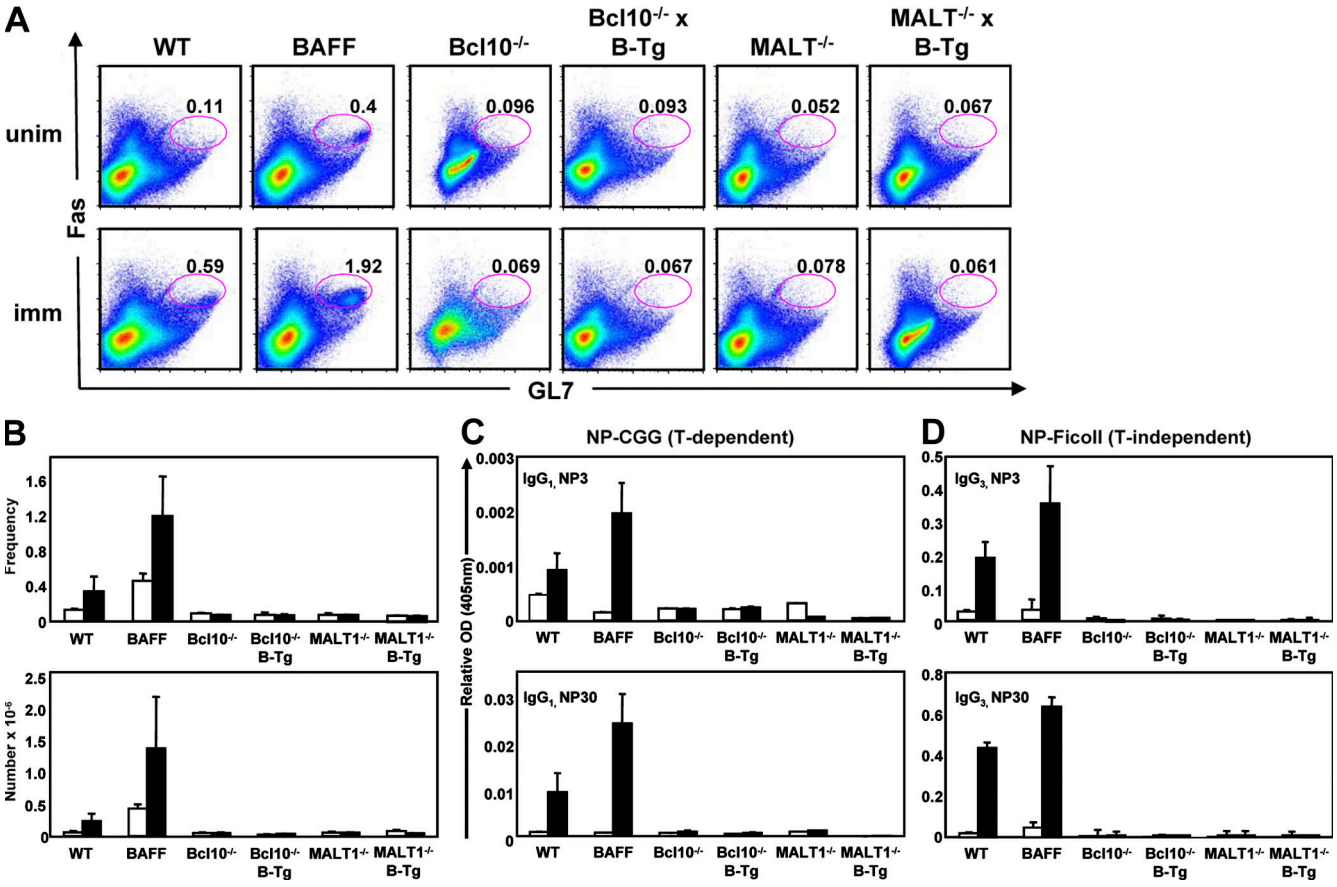

Figure 6. Td and Ti humoral responses are dysfunctional in the absence of MALT1. (A and B) Mice of the indicated genotypes (n = 4 mice/genotype) were left unimmunized (unim) or immunized (imm) with the Td antigen NP-CGG. GC B cells in the spleens of these mice were detected by immunostaining plus flow cytometry (percentages are shown). The quantification of the results of two such independent analyses are shown in B. Mice immunized with (C) the Td antigen NP-CGG or (D) the Ti antigen NP-Ficoll were analyzed by sandwich ELISA for the presence of low affinity (NP-30) and high affinity (NP-3) anti-NP antibodies. One out of two representative experiments is shown (n = 4 mice/genotype for each experiment). For B–D, white bars represent unimmunized controls and black bars represent immunized mice.

DISCUSSION

Although modest defects in signaling downstream of the BCR have been reported for MALT1$^{-/-}$ mice (Ferch et al., 2007), we find that these defects do not impinge on B cell activation in terms of IgM-induced proliferation, NF-κB activation, or B7 up-regulation. Nevertheless, MZ B cells as well as serum Ig titers are significantly decreased in our MALT1$^{-/-}$ mice, implying that B cell survival signals other than those mediated by the BCR require MALT1. Because BAFF overexpression has been reported to drive the expansion of MZ B cells, as well as to support GC responses and induce class switch recombination, we investigated whether MALT1 plays a role in BAFF signaling (Kalled, 2006).

We demonstrate for the first time that MALT1 is integrated in a novel signaling pathway induced by BAFF, and MALT1 is necessary for the full manifestation of BAFF-dependent in vivo effects. Specifically, we show that BAFF-induced phosphorylation of NF-κB2 (p100) in FO and MZ B cells is dependent on MALT1. Furthermore, we demonstrate that BAFF-induced degradation of p100 and RelB nuclear translocation is diminished in the absence of MALT1. BAFF-induced signaling events can also be arrested in the BJAB cell line by siRNA-mediated knockdown of MALT1, thus corroborating our findings in the knockout mice. Because this cell line is derived from a human Burkitt's lymphoma, MALT1 may also play a role in BAFF activation of NF-κB2 in the human system. Based on the block in B cell maturation in the MALT1$^{-/-}$ mice and the fact that signals downstream of the BAFF-R are necessary for B cell survival, we place this signaling node downstream of the BAFF-R rather than TACI or BCMA, which are also know to bind BAFF (Marsters et al., 2000; Thompson et al., 2000; Wu et al., 2000; Thompson et al., 2001; Yan et al., 2001; Ruefli-Brasse et al., 2003; Ruland et al., 2003). The observation that siRNA-mediated MALT1 knockdown in the BJAB cell line, which only expresses BAFF-R, arrests BAFF-induced signal transduction corroborates this notion (Thompson et al., 2001).

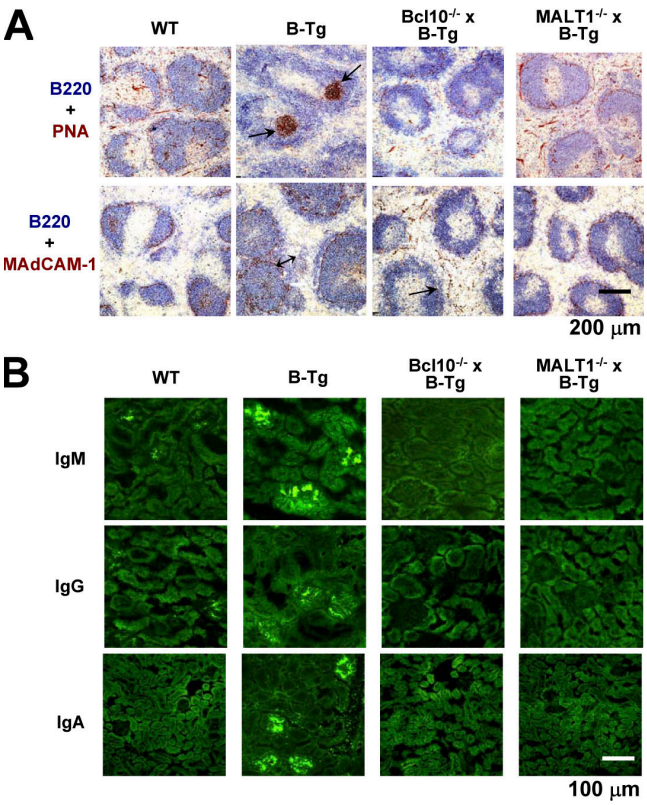

Figure 7. BAFF-induced GC formation in the spleen and Ig deposition in the kidney require MALT1. (A) Spleen sections from mice of the indicated genotypes were immunostained to detect B220 plus the GC marker PNA (top) or B220 plus the MZ sinus marker MAdCAM-1 (bottom). Arrows indicate PNA$^+$ GC B cells. (B) Kidney sections from the mice in A were stained with FITC-conjugated antibodies specific for the indicated Ig isotypes and visualized using fluorescence microscopy. Images shown are representative of four independent analyses of at least eight mice/genotype.

Although MALT1 is essential for BAFF-driven NF-κB2 activation in all B cell subsets, the requirement for MALT1 for BAFF-mediated B cell survival is only manifested in MZ B cells. Specifically, in response to BAFF stimulation, MALT1$^{-/-}$ FO B cells exhibited normal BAFF-stimulated survival in vitro accompanied by up-regulation of Bcl-2, Bcl-xL, and cyclin D1, yet all of these readouts are MALT1 dependent in MZ B cells. The only exception to this pattern was in the case of cyclin D2 that seems to require MALT1 in both MZ and FO B cell subsets, suggesting that there are other cell-cycle entry mediators that compensate for cyclin D2 in MALT$^{-/-}$ FO B cells. Our findings potentially explain why MALT1$^{-/-}$ as well as RelB$^{-/-}$ and *aly/aly* mice do not phenocopy BAFF$^{-/-}$ mice but share some similarities (Shinkura et al., 1999; Weih et al., 2001). The reason for the incomplete phenocopy is likely because the MALT1– NF-κB2 axis induces an essential BAFF-mediated survival program in MZ B cells that is redundant in FO B cells. Indeed, mice with B cell–specific ablation of TRAF2/3 and constitutive activation of the alternative NF-κB pathway have a preferentially expanded MZ B cell compartment, suggesting that MZ B cells are particularly sensitive to TRAF3 degradation. Indeed, TRAF3 levels have been shown to be low in FO B cells (Gardam et al., 2008), suggesting that this adaptor (and by extension NF-κB2 signaling) may be more relevant for the "fine tuning" of BAFF-R signals in the MZ compartment. The phosphoinositide 3-kinase (PI3-kinase) pathway is a possible candidate for the alternative BAFF-dependent survival pathway that sustains MALT1$^{-/-}$ FO B cells (Patke et al., 2006). In support of this concept, we found that pharmacologic inhibition of p110δ abrogated the BAFF-dependent survival of WT and MALT1$^{-/-}$ FO B cells with relatively little effect on MZ B cells (Fig. S5). Another possibility is that Bcl10 could compensate for the absence of MALT1 in FO B cells. Indeed, we have observed defects in BAFF-induced signaling and survival in Bcl10$^{-/-}$ B220$^+$ B cells (unpublished data). The fact that Bcl10$^{-/-}$ mice have a defect in FO B cell development as well as MZ development lends credence to this hypothesis.

BAFF-Tg mice exhibit pathological features such as hyperglobulinemia, spontaneous GC formation, and Ig deposition in the kidneys (Mackay et al., 1999), and we show that this

phenotype does not occur in the absence of MALT1. In addition, the expansion of the B1 B cell compartment in the peritoneum has also been reported in BAFF-Tg animals, albeit to varying degrees in different studies (Mackay et al., 1999; Khare et al., 2000; Gavin et al., 2005). In our hands, we see reproducible increases in the B1 B cell population in the presence of the BAFF transgene that are ablated in the context of either MALT1 or Bcl10 deficiency. In addition, the increase in MZ B cells typically found in BAFF-Tg mice critically requires MALT1. GC B cell maintenance and Ig class switching depend on BAFF-R signaling (Kalled, 2006). Interestingly, some Ig titers are decreased in MALT1$^{-/-}$ mice, as well as the GC response to antigen (Figs. 5 A and 6 A). These were not corrected by excess BAFF, further supporting a role for MALT1 in BAFF-R signaling. Because GC responses are seeded by FO B cells, we hypothesize that as FO B cells become activated and rapidly proliferate within the GC niche, other BAFF-mediated survival programs that normally support FO B cell survival, such as PI3-kinase activation, are no longer sufficient within this highly cytotoxic milieu. Therefore, like MZ B cells, GC B cells may require MALT1-dependent alternative NF-κB activation in response to BAFF stimulation.

Because both Bcl10 and MALT1 are required for TCR signaling, it was important to determine whether Bcl10 and MALT1 functions were required in B cells themselves for these BAFF-induced effects. In addition, BAFF has been known to have a co-stimulatory effect on T cells, and the defect in Td antigen response we observe in MALT1$^{-/-}$ mice could be caused by this effect (Mackay and Leung, 2006). Indeed, using mixed bone marrow chimeric BAFF-Tg × $J_h^{-/-}$ mice that contain WT T cells and knockout B cells, we found that BAFF-induced increases in GC formation and kidney Ig deposition as well as the elevation of global Ig and antigen-specific Ig all require B cell–intrinsic expression of MALT1 (and Bcl10; Figs. S6 and S7). Therefore, MALT1 must be expressed in B cells to mediate BAFF-driven effects in vivo.

Given that BCR-mediated proliferation and canonical NF-κB activation are intact in MALT1$^{-/-}$ mice (Fig. 1), the absences of MZ B and B1 cells in these mice are likely not caused by a lesion in BCR signaling, and our data strongly suggest that these defects are caused by impaired NF-κB2 activation downstream of BAFF-R. However, the possibility exists that an unknown factor is nonfunctional in MALT1$^{-/-}$ mice and generates a phenotype that cannot be rescued by BAFF overexpression. The reported block in MALT1$^{-/-}$ mice of the activation of c-Rel–containing NF-κB heterodimers in response to BCR signaling could represent such a possibility (Ferch et al., 2007). In contrast, Bcl10$^{-/-}$ mice exhibit nonfunctional NF-κB signaling, B cell proliferation, and a CD23^{low} compartment that is dominated by T1 (CD21^{low}) B cells, suggesting an underlying BCR lesion (Figs. 1 and 5 B). Therefore, it is impossible to tell whether the lack of MZ and B1 B cells in Bcl10$^{-/-}$ mice is caused by perturbations downstream of the BCR or signaling defects in the BAFF-induced noncanonical NF-κB pathway. Sasaki et al. (2006) report that constitutively active canonical NF-κB signaling in B cells can rescue MZ and FO B cell development in a BAFF-R$^{-/-}$ background. The implication is that in situations of enforced activation of BAFF- or BCR-initiated pathways, BAFF and BCR signaling activities can compensate for one another.

A recent report revealed that c-IAP1/2 acts as an E3 ubiquitin ligase and polyubiquitinates NIK in a Lys-48–dependent manner. c-IAP1/2 is brought in proximity to TRAF3 via TRAF2, and TRAF3 in turn links this complex with NIK. Stabilization of NIK is achieved by recruitment of the complex to the membrane upon receptor aggregation, resulting in a TRAF2-dependent activation of c-IAP1/2 that induces the K48-mediated ubiquitination of TRAF3 and its degradation. TRAF3 degradation allows for NIK to be relieved from this complex so that it may initiate alternative NF-κB signaling (Vallabhapurapu et al., 2008). Interestingly, we have found that MALT1 and TRAF3 coassociate in BJAB cells and primary mouse B cells (Fig. 4, B and C). We propose that MALT1 serves as a scaffold for c-IAP1/2, TRAF2, and TRAF3, with TRAF3 in turn binding to NIK. However, this scaffold may not be necessary for the constitutive activity of c-IAP1/2 on NIK itself. In contrast, upon receptor activation, the MALT1 scaffold may play an important role in allowing c-IAP1/2 to polyubiquitinate TRAF3 on K48, leading to its degradation. In agreement with this possibility, we have observed that TRAF3 is elevated in MZ B cells obtained from MALT1$^{-/-}$ mice (Fig. 4 A). Furthermore, upon BAFF stimulation, we found that the TRAF3–MALT1 complex dissociates, keeping with the notion that TRAF3 is rapidly degraded after BAFF-R signaling. There are two possibilities for how MALT1 may function after receptor activation: either MALT1 encourages TRAF2 to activate c-IAP1/2 by bringing them into closer proximity while recruited to the activated BAFF-R, or alternatively MALT1, perhaps through a protein conformational change that occurs upon cell signaling, may bring activated c-IAP1/2 into closer proximity with TRAF3 itself. Either scenario would promote TRAF3 degradation and the activation of NF-κB2. Future experiments will be designed to distinguish between these possibilities.

Both Bcl10 and MALT1 are frequently involved in translocations associated with extranodal MZ B cell lymphomas of mucosa-associated lymphoid tissues (MALT lymphomas; Akagi et al., 1999; Dierlamm et al., 1999; Willis et al., 1999; Zhang et al., 1999). However, mice transgenic for the API2–MALT1 translocation do not develop lymphoma after 50 wk, implying that the presence of the fusion protein alone is not sufficient to drive neoplastic progression (Baens et al., 2006). BAFF levels are elevated in the serum of patients with a variety of B cell malignancies (Ng et al., 2005), and autocrine BAFF production is crucial for the survival of some B cell lymphomas (Fu et al., 2006). One possibility is that MALT lymphomagenesis is driven by MALT1 translocations because they dysregulate BAFF activity. It would be intriguing to investigate whether MALT lymphoma patients have elevated BAFF levels in their serum.

In summary, we have shown both in vitro and in vivo that MALT1 is crucial for many of the biological effects mediated by BAFF. Our results suggest that MALT1 is a critical intermediate

in a novel signaling pathway emanating from BAFF-R, which drives the survival and expansion of MZ B cells. MALT1 may thus represent an attractive target for therapeutic intervention in the treatment of lymphoma or autoimmunity.

MATERIALS AND METHODS

Mice. The generation of Bcl10$^{-/-}$, MALT1$^{-/-}$, and BAFF-Tg mice was described previously (Mackay et al., 1999; Ruland et al., 2001, 2003). BAFF-Tg mice were provided by J. Browning and A. Ranger (Biogen Idec, Cambridge, MA). Bcl10$^{-/-}$ × BAFF-Tg and MALT1$^{-/-}$ × BAFF-Tg mice were maintained with the transgene expressed heterozygously to generate littermate controls. BAFF-Tg$^{+/-}$ and BAFF-Tg$^{+/+}$ mice have equivalent phenotypes (McCarthy et al., 2006). $J_h^{-/-}$ mice were obtained from S. Fillatreau (Deutsches Rheuma-Forschungszentrum, Berlin, Germany; Gu et al., 1993). Mice were analyzed at 8–10 wk of age. All animal experiments were conducted using protocols approved by the Animal Use Committee of the University of Toronto.

Proliferation. Spleens from WT, Bcl10$^{-/-}$, and MALT1$^{-/-}$ mice were homogenized and erythrocytes were removed using Red Blood Cell Lysing Buffer (Sigma-Aldrich). B220$^+$ B cells were isolated by negative depletion using biotinylated anti-CD11b, anti–Thy 1.2, and anti-Ter119 antibodies plus streptavidin-conjugated magnetic beads (BD). Purity of B220$^+$ cells was confirmed to be >95% using flow cytometry. 2×10^5 cells per well were cultured in 96-well plates in RPMI 1640 medium supplemented with 10% FCS, 5 mM L-glutamine, 55 μM 2-mercaptoethanol, and antibiotics, and stimulated with the indicated doses of anti-IgM (Jackson ImmunoResearch Laboratories) or anti-CD40 (clone 3/23; BD) for the times indicated in Fig. 1 and Fig. S1. 1 μCi [^{3}H]thymidine (PerkinElmer) was added for the last 8 h of culture. Proliferation was measured using a microplate scintillation counter (Top Count NXT; Packard).

Immunoblotting. B cells were serum-starved for 4 h and stimulated in OptiMEM medium with or without 2 μg/ml recombinant BAFF (PeproTech) at 37°C for the times indicated in the figures. For anti-IgM or CD40L treatment, starved B cells were stimulated with 5 μg/ml anti–mouse IgM or 250 ng/ml soluble CD40L (PeproTech) for the indicated times, respectively. For the preparation of cytosolic extracts, cells were resuspended in lysis buffer (50 mM Tris-Cl [pH 7.4], 250 mM NaCl, 1 mM EDTA, 1% NP-40, 1 mM PMSF, 1 mM NaF, 1 mM Na_4VO_3, and complete protease inhibitor cocktail [Roche]). For the preparation of nuclear lysates, cells were resuspended in buffer A (10 mM Hepes [pH 7.4], 10 mM KCl, 0.1 mM EDTA supplemented with 1 mM PMSF, 1 mM dithiothreitol, and phosphatase and protease inhibitor cocktails [Roche]), for 15 min on ice with occasional agitation. NP-40 was added to a final concentration of 0.65% and incubated for a further 15 min on ice. Samples were centrifuged at 10,000 rpm for 1 min at 4°C to pellet nuclei. Nuclear pellets were resuspended in buffer C (20 mM Hepes [pH 7.9], 0.4 M NaCl, 1 mM EDTA, and 1 mM EGTA supplemented as described) for 30 min on ice with occasional agitation. Lysates were cleared by centrifugation, at 14,000 rpm for 10 min at 4°C, normalized for protein content, and Western blotted according to standard protocols. Blots were probed with the indicated antibodies and visualized using enhanced chemiluminescence according to the manufacturer's protocol (GE Healthcare). Blots were stripped and reprobed with antitubulin or antiactin antibodies (Sigma-Aldrich) as a loading control. Antibodies against IκBα, NF-κB2 (p100/p52), RelB, and phospho-p100 (Ser 866/870) were obtained from Cell Signaling Technology. Antibodies against MALT1, PKCδ, lamin A, TRAF2, and TRAF3 were obtained from Santa Cruz Biotechnology, Inc.

EMSA. B cells were serum starved and stimulated for 8 h in 5 μg/ml anti-IgM, and nuclear extracts were prepared as described. 2.5-μg nuclear lysate samples were analyzed for DNA binding using an EMSA kit (Odyssey IR; LI-COR Biosciences). For supershift assays, 1 μl anti-p65 (Santa Cruz Biotechnology, Inc.) was added to a DNA binding reaction before addition of labeled oligo and was incubated at room temperature for 20 min. Binding reactions were fractionated on TBE gels (Bio-Rad Laboratories) and visualized using an Odyssey infrared imager.

B cell survival assays. MZ (CD21^{high}CD23^{low}), FO (CD21^{low}CD23^{high}), and T2 (CD21^{high}HSA^{high}) B cells were isolated from total B220$^+$ B cells using a cell sorter (FACSAria; BD). FACS-sorted B cells were cultured for 72 h with or without 2 μg/ml of recombinant BAFF. Unfractionated B220$^+$ B cells were cultured with BAFF for the times indicated in the figures. 5 μg/ml anti-IgM was used in survival studies for the indicated times. Viability was assessed using annexin V/PI staining and acquired on a flow cytometer (FACSCalibur; BD). Survival was expressed as the fold increase in viable cells over untreated controls, or as the percentage of viable cells. IC87114 (a gift from K. Okkenhaug, Babraham Institute, Cambridge, England, UK) was resuspended in DMSO and used at a final concentration of 15 μM.

Serum Ig ELISA. Ig isotypes were determined using standard ELISA of serially diluted mouse serum samples. Primary antibodies recognizing mouse Igs and horseradish peroxidase (HRP)–linked secondary antibodies recognizing specific isotypes were obtained from SouthernBiotech. Ig standards were from eBioscience.

Flow cytometry. Peritoneal lavage was conducted by injecting 8 ml PBS into the peritoneum of a euthanized mouse and massaging gently for 2 min. Recovered peritoneal cells were resuspended in FACS buffer and incubated with anti-CD11b–FITC, anti-B220–allophycocyanin (APC; both from eBioscience), anti-CD5–PE, and anti-IgM–Cyc (both from BD). Immunostained cells were washed in FACS buffer and resuspended in 2% paraformaldehyde. Total splenocytes were collected from spleens as described, resuspended in FACS buffer, and incubated with anti-CD21–FITC, anti-IgM–CyC, anti-B220–PE (all from BD), anti-CD1d–PE, and anti-CD23–biotin followed by incubation with streptavidin-APC (all from eBioscience). For BAFF-R staining, whole splenocytes were incubated with anti-CD4–PE, anti-B220–FITC (both from BD), and BAFF-R–biotin (the gift of S. Kalled, Biogen Idec, Cambridge, MA), followed by incubation with streptavidin-APC. For B7 upregulation experiments, splenocytes were incubated with a cocktail consisting of B220-PerCP, CD21-FITC, CD23-PE, and B7.1/B7.2 (CD80/86)-APC (all from BD). Immunostained splenocytes were washed in FACS buffer and resuspended in 2% paraformaldehyde. Samples were processed using a FACSCalibur and analyzed using FlowJo software (Tree Star, Inc.).

Immunoprecipitation. Cells were treated with stimulus and washed once with cold PBS. Cells were resuspended in 1 ml of modified RIPA buffer (50 mM Tris-Cl [pH 7.4], 1% NP-40, 0.25% Na-deoxycholate, 150 mM NaCl, 1 mM EDTA, 1 mM PMSF, and protease and phosphatase inhibitor cocktail tablets), incubated at 4°C with constant rotation, and centrifuged to remove debris. Lysates were precleared by adding 30 μl Protein G Sepharose 4 Fast Flow (GE Healthcare) and rotating at 4°C for 30 min. Precleared lysates were incubated with a 1:100 dilution of anti-MALT1 (Santa Cruz Biotechnology, Inc.) and overnight at 4°C with constant rotation. Immunocomplexes were precipitated with 30 μl Protein G Sepharose 4 Fast Flow with rotation at 4°C for 30 min, eluted by boiling in Laemmli buffer, fractionated on SDS-PAGE gels, and immunoblotted according to standard protocols.

Intracellular phospho-flow cytometry. 5×10^5 B220$^+$ B cells or BJAB cells were stimulated at 37°C with 2 μg/ml BAFF or MegaAPRIL (Enzo Life Sciences, Inc.) for the times indicated in the figures. Cells were fixed with paraformaldehyde and permeablized in 1 ml Phosphoflow Perm Buffer III (90% methanol based; BD). After washing, cells were stained with an antibody cocktail consisting of 1:100 dilutions of anti-CD21–PE, anti-CD23–FITC (both from BD), and anti–phospho-p100 (Ser 866/870), and incubated on ice for 30 min. After washing in FACS buffer (PBS containing 3%FCS and 0.09% sodium azide), cells were stained with a 1:1,000 dilution of anti–rabbit Alexa Fluor 647 (Molecular Probes) for 1 h on ice. Cells were washed, resuspended in FACS buffer, and acquired using a flow cytometer (FACSCanto; BD). Samples were analyzed using FlowJo software.

RNAi-mediated knockdown. BJAB human Burkitt lymphoma cells (the gift of S. Kalled) were maintained in RPMI 1640 media supplemented as described. 5×10^6 cells were washed and resuspended in 100 µl Nucleofector Solution T (Lonza) with 125 pmol siGenome SMARTpool MALT1 siRNA or NF-κB2 siRNA (Thermo Fisher Scientific), and nucleofected using program T-016 on a Nucleofector II device (Lonza). Cells were collected for analysis 48 h after nucleofection.

Real-time PCR. FO and MZ B cells were FACS sorted as described, stimulated with BAFF for 12 h as described, and lysed in TRIzol reagent (Invitrogen), and RNA was isolated using the manufacturer's protocol. cDNA was synthesized using 500 ng RNA, oligo$(dT)_{20}$ primers, and a cDNA first-strand synthesis kit (Invitrogen). cDNAs were amplified using Power SYBR Green PCR Master Mix (Applied Biosystems) on a real-time PCR system (ABI 7900T; Applied Biosystems) and were normalized against GAPDH as an internal control. Data were expressed as fold increase over unstimulated controls.

Td and Ti humoral responses. For assessment of Td responses, 100 µg NP-CCG (Biosearch Technologies) was mixed 1:1 with imject alum (Thermo Fisher Scientific) and administered i.p. Spleens and serum were harvested at 11 d after immunization. GC B cells in the $B220^+$ population of the spleen were assessed using anti-GL7–FITC and anti-Fas–biotin (both from eBioscience), followed by streptavidin-CyC (BD). The production of high and low affinity anti-NP antibodies was assessed by applying serum to ELISA plates coated with either NP_{30} or NP_3 (Biosearch Technologies). Detection was performed using the secondary reagents described for serum Ig ELISAs. For assessment of Ti responses, 30 µg NP-Ficoll (Biosearch Technologies) was administered i.p., and spleens and serum were harvested and analyzed at 7 d after immunization as described for Td responses.

Immunohistochemistry and immunofluorescence. Immunohistochemistry and immunofluorescence were performed as previously described (McCarthy et al., 2006). In brief, spleen sections were stained with PNA-biotin (Vector Laboratories) plus anti-B220–FITC to detect GCs, or with MAdCAM-1–biotin (eBioscience) plus anti-B220–FITC to visualize the MZ. Sections were washed and incubated with streptavidin-HRP (Prozyme) and anti-FITC–alkaline phosphatase (Roche). Colorimetric development was conducted using NovaRED HRP and Alkaline Phosphatase Substrate development kits (Vector Laboratories) according to the manufacturer's protocols. Deposition of various Ig isotypes in the kidneys was visualized by staining with anti-IgA–FITC, anti-IgM–FITC, or anti-IgG–FITC (BD). Images of stained sections were acquired using a digital fluorescent microscope (model DMR; Leica) and Openlab software (PerkinElmer).

Bone marrow chimeras. Recipient mice were lethally irradiated by two exposures to 550 rad before injection in the tail vein of 10^6 mixed (1:1) bone marrow cells. Irradiated, transplanted mice were fed drinking water containing 2 mg/ml neomycin sulfate (Bioshop Canada Inc.) for 2 wk. After 10–12 wk of bone marrow reconstitution, serum Ig analysis, B cell subset analysis, immunohistochemistry, and immunofluorescence were conducted as described.

Statistical analysis. Statistical analyses were conducted using the Student's *t* test for variance.

Online supplemental material. Table S1 shows absolute numbers of B cells in the spleen and peritoneum. Table S2 shows oligos used in real-time PCR analysis. Fig. S1 shows BAFF-R expression on various B cell subsets from the indicated genotypes. Shaded histograms indicate isotype control staining. Fig. S2 (A and B) shows IκBα degradation and p100 processing, respectively, in response to CD40L in $MALT1^{+/+}$ and $MALT1^{-/-}$ B cells. Fig. S3 shows the sorting strategy for MZ and FO B cells from $B220^+$ B cells using CD21 and CD23. Fig. S4 A shows the viability of purified $MALT1^{+/+}$ and $MALT1^{-/-}$ $B220^+$ B cells with or without BAFF treatment Fig. S4 (B and C) shows anti-IgM–induced survival and B7.2 up-regulation in T2 B cells, respectively, sorted from $MALT1^{+/+}$ and $MALT1^{-/-}$ mice. Fig. S5 shows the effect of p110δ inhibition on BAFF induced survival on MZ and FO B cells from the indicated genotypes. Fig. S6 A shows basal serum Ig levels of mixed bone marrow chimeric mice from the indicated genotypes. WT+$J_h^{-/-}$→WT denotes WT bone marrow mixed with $J_h^{-/-}$ bone marrow, introduced into a WT lethally irradiated recipient. Fig. S6 B shows immunohistochemical and immunofluorescence analysis of spleen and kidney sections, respectively, of mixed bone marrow chimeric mice from the indicated genotype. Fig. S7 A shows GC B cell frequencies in the spleens of the indicated genotypes of mixed bone marrow chimeric mice that had been left unimmunized (white bars) and immunized with Td antigen NP-CGG (black bars). Fig. S7 B shows NP-CGG (Td) antibody titers in mixed bone marrow chimeric mice. Online supplemental material is available at http://www.jem.org/cgi/content/full/jem.20091802/DC1.

We wish to acknowledge the assistance of C. Smith of the Medical Sciences Building, and R. Nayyer and F. Tong of the Princess Margaret Hospital flow cytometry facilities, respectively. We thank Drs. A. Ranger and J. Browning of Biogen Idec for BAFF-Tg mice, and Dr. S. Kalled of Biogen Idec for anti–BAFF-R antibody and the BJAB cell line. We thank Dr. K. Okkenhaug at the Babraham Institute for the p110δ inhibitor. We are grateful to Dr. Z. Hao, Dr. M. Lechmann, Dr. M. Pellegrini, and Mr. G. Duncan for critical reading of the manuscript and helpful advice, and to Dr. M. Saunders for scientific editing.

This work was supported by a Terry Fox Cancer Foundation Grant to T.W. Mak, a Canadian Institutes of Health Research operating grant (MOP 67157) to J.L. Gommerman, and a Natural Sciences and Engineering Research Council of Canada studentship to M.W. Tusche.

The authors have no conflicting financial interests.

Submitted: 18 August 2009
Accepted: 20 October 2009

REFERENCES

Akagi, T., M. Motegi, A. Tamura, R. Suzuki, Y. Hosokawa, H. Suzuki, H. Ota, S. Nakamura, Y. Morishima, M. Taniwaki, and M. Seto. 1999. A novel gene, MALT1 at 18q21, is involved in t(11;18) (q21;q21) found in low-grade B-cell lymphoma of mucosa-associated lymphoid tissue. *Oncogene*. 18:5785–5794. doi:10.1038/sj.onc.1203018

Baens, M., S. Fevery, X. Sagaert, H. Noels, S. Hagens, V. Broeckx, A.D. Billiau, C. De Wolf-Peeters, and P. Marynen. 2006. Selective expansion of marginal zone B cells in Emicro-API2-MALT1 mice is linked to enhanced IkappaB kinase gamma polyubiquitination. *Cancer Res.* 66:5270–5277. doi:10.1158/0008-5472.CAN-05-4590

Batten, M., J. Groom, T.G. Cachero, F. Qian, P. Schneider, J. Tschopp, J.L. Browning, and F. Mackay. 2000. BAFF mediates survival of peripheral immature B lymphocytes. *J. Exp. Med.* 192:1453–1466. doi:10.1084/jem.192.10.1453

Claudio, E., K. Brown, S. Park, H. Wang, and U. Siebenlist. 2002. BAFF-induced NEMO-independent processing of NF-kappa B2 in maturing B cells. *Nat. Immunol.* 3:958–965. doi:10.1038/ni842

Dierlamm, J., M. Baens, I. Wlodarska, M. Stefanova-Ouzounova, J.M. Hernandez, D.K. Hossfeld, C. De Wolf-Peeters, A. Hagemeijer, H. Van den Berghe, and P. Marynen. 1999. The apoptosis inhibitor gene API2 and a novel 18q gene, MLT, are recurrently rearranged in the t(11;18)(q21;q21) associated with mucosa-associated lymphoid tissue lymphomas. *Blood*. 93:3601–3609.

Ferch, U., C.M. zum Büschenfelde, A. Gewies, E. Wegener, S. Rauser, C. Peschel, D. Krappmann, and J. Ruland. 2007. MALT1 directs B cell receptor-induced canonical nuclear factor-kappaB signaling selectively to the c-Rel subunit. *Nat. Immunol.* 8:984–991. doi:10.1038/ni1493

Fu, L., Y.C. Lin-Lee, L.V. Pham, A. Tamayo, L. Yoshimura, and R.J. Ford. 2006. Constitutive NF-kappaB and NFAT activation leads to stimulation of the BLyS survival pathway in aggressive B-cell lymphomas. *Blood*. 107:4540–4548. doi:10.1182/blood-2005-10-4042

Gardam, S., F. Sierro, A. Basten, F. Mackay, and R. Brink. 2008. TRAF2 and TRAF3 signal adapters act cooperatively to control the maturation and survival signals delivered to B cells by the BAFF receptor. *Immunity*. 28:391–401. doi:10.1016/j.immuni.2008.01.009

Gavin, A.L., B. Duong, P. Skog, D. Aït-Azzouzene, D.R. Greaves, M.L. Scott, and D. Nemazee. 2005. deltaBAFF, a splice isoform of BAFF, opposes full-length BAFF activity in vivo in transgenic mouse models. *J. Immunol.* 175:319–328.

Gu, H., Y.R. Zou, and K. Rajewsky. 1993. Independent control of immunoglobulin switch recombination at individual switch regions evidenced through Cre-loxP-mediated gene targeting. *Cell*. 73:1155–1164. doi:10.1016/0092-8674(93)90644-6

Hayden, M.S., and S. Ghosh. 2004. Signaling to NF-kappaB. *Genes Dev*. 18:2195–2224. doi:10.1101/gad.1228704

Huang, X., M. Di Liberto, A.F. Cunningham, L. Kang, S. Cheng, S. Ely, H.C. Liou, I.C. Maclennan, and S. Chen-Kiang. 2004. Homeostatic cell-cycle control by BLyS: Induction of cell-cycle entry but not G1/S transition in opposition to p18INK4c and p27Kip1. *Proc. Natl. Acad. Sci. USA*. 101:17789–17794. doi:10.1073/pnas.0406111101

Kalled, S.L. 2006. Impact of the BAFF/BR3 axis on B cell survival, germinal center maintenance and antibody production. *Semin. Immunol*. 18:290–296. doi:10.1016/j.smim.2006.06.002

Kayagaki, N., M. Yan, D. Seshasayee, H. Wang, W. Lee, D.M. French, I.S. Grewal, A.G. Cochran, N.C. Gordon, J. Yin, et al. 2002. BAFF/BLyS receptor 3 binds the B cell survival factor BAFF ligand through a discrete surface loop and promotes processing of NF-kappaB2. *Immunity*. 17:515–524. doi:10.1016/S1074-7613(02)00425-9

Khare, S.D., I. Sarosi, X.Z. Xia, S. McCabe, K. Miner, I. Solovyev, N. Hawkins, M. Kelley, D. Chang, G. Van, et al. 2000. Severe B cell hyperplasia and autoimmune disease in TALL-1 transgenic mice. *Proc. Natl. Acad. Sci. USA*. 97:3370–3375. doi:10.1073/pnas.050580697

Li, Q., and I.M. Verma. 2002. NF-kappaB regulation in the immune system. *Nat. Rev. Immunol*. 2:725–734. doi:10.1038/nri910

Ling, L., Z. Cao, and D.V. Goeddel. 1998. NF-kappaB-inducing kinase activates IKK-alpha by phosphorylation of Ser-176. *Proc. Natl. Acad. Sci. USA*. 95:3792–3797. doi:10.1073/pnas.95.7.3792

Mackay, F., and H. Leung. 2006. The role of the BAFF/APRIL system on T cell function. *Semin. Immunol*. 18:284–289. doi:10.1016/j.smim.2006.04.005

Mackay, F., S.A. Woodcock, P. Lawton, C. Ambrose, M. Baetscher, P. Schneider, J. Tschopp, and J.L. Browning. 1999. Mice transgenic for BAFF develop lymphocytic disorders along with autoimmune manifestations. *J. Exp. Med*. 190:1697–1710. doi:10.1084/jem.190.11.1697

Marsters, S.A., M. Yan, R.M. Pitti, P.E. Haas, V.M. Dixit, and A. Ashkenazi. 2000. Interaction of the TNF homologues BLyS and APRIL with the TNF receptor homologues BCMA and TACI. *Curr. Biol*. 10:785–788. doi:10.1016/S0960-9822(00)00566-2

McCarthy, D.D., S. Chiu, Y. Gao, L.E. Summers-deLuca, and J.L. Gommerman. 2006. BAFF induces a hyper-IgA syndrome in the intestinal lamina propria concomitant with IgA deposition in the kidney independent of LIGHT. *Cell. Immunol*. 241:85–94. doi:10.1016/j.cellimm.2006.08.002

Nardelli, B., O. Belvedere, V. Roschke, P.A. Moore, H.S. Olsen, T.S. Migone, S. Sosnovtseva, J.A. Carrell, P. Feng, J.G. Giri, and D.M. Hilbert. 2001. Synthesis and release of B-lymphocyte stimulator from myeloid cells. *Blood*. 97:198–204. doi:10.1182/blood.V97.1.198

Ng, L.G., C.R. Mackay, and F. Mackay. 2005. The BAFF/APRIL system: life beyond B lymphocytes. *Mol. Immunol*. 42:763–772. doi:10.1016/j.molimm.2004.06.041

Oliver, A.M., F. Martin, G.L. Gartland, R.H. Carter, and J.F. Kearney. 1997. Marginal zone B cells exhibit unique activation, proliferative and immunoglobulin secretory responses. *Eur. J. Immunol*. 27:2366–2374. doi:10.1002/eji.1830270935

Patke, A., I. Mecklenbräuker, H. Erdjument-Bromage, P. Tempst, and A. Tarakhovsky. 2006. BAFF controls B cell metabolic fitness through a PKCβ- and Akt-dependent mechanism. *J. Exp. Med*. 203:2551–2562. doi:10.1084/jem.20060990

Ruefli-Brasse, A.A., D.M. French, and V.M. Dixit. 2003. Regulation of NF-kappaB-dependent lymphocyte activation and development by paracaspase. *Science*. 302:1581–1584. doi:10.1126/science.1090769

Ruland, J., G.S. Duncan, A. Elia, I. del Barco Barrantes, L. Nguyen, S. Plyte, D.G. Millar, D. Bouchard, A. Wakeham, P.S. Ohashi, and T.W. Mak. 2001. Bcl10 is a positive regulator of antigen receptor-induced activation of NF-kappaB and neural tube closure. *Cell*. 104:33–42. doi:10.1016/S0092-8674(01)00189-1

Ruland, J., G.S. Duncan, A. Wakeham, and T.W. Mak. 2003. Differential requirement for Malt1 in T and B cell antigen receptor signaling. *Immunity*. 19:749–758. doi:10.1016/S1074-7613(03)00293-0

Sasaki, Y., S. Casola, J.L. Kutok, K. Rajewsky, and M. Schmidt-Supprian. 2004. TNF family member B cell-activating factor (BAFF) receptor-dependent and -independent roles for BAFF in B cell physiology. *J. Immunol*. 173:2245–2252.

Sasaki, Y., E. Derudder, E. Hobeika, R. Pelanda, M. Reth, K. Rajewsky, and M. Schmidt-Supprian. 2006. Canonical NF-kappaB activity, dispensable for B cell development, replaces BAFF-receptor signals and promotes B cell proliferation upon activation. *Immunity*. 24:729–739. doi:10.1016/j.immuni.2006.04.005

Schiemann, B., J.L. Gommerman, K. Vora, T.G. Cachero, S. Shulga-Morskaya, M. Dobles, E. Frew, and M.L. Scott. 2001. An essential role for BAFF in the normal development of B cells through a BCMA-independent pathway. *Science*. 293:2111–2114. doi:10.1126/science.1061964

Schneider, P. 2005. The role of APRIL and BAFF in lymphocyte activation. *Curr. Opin. Immunol*. 17:282–289. doi:10.1016/j.coi.2005.04.005

Schneider, P., F. MacKay, V. Steiner, K. Hofmann, J.L. Bodmer, N. Holler, C. Ambrose, P. Lawton, S. Bixler, H. Acha-Orbea, et al. 1999. BAFF, a novel ligand of the tumor necrosis factor family, stimulates B cell growth. *J. Exp. Med*. 189:1747–1756. doi:10.1084/jem.189.11.1747

Senftleben, U., Y. Cao, G. Xiao, F.R. Greten, G. Krähn, G. Bonizzi, Y. Chen, Y. Hu, A. Fong, S.C. Sun, and M. Karin. 2001. Activation by IKKalpha of a second, evolutionary conserved, NF-kappa B signaling pathway. *Science*. 293:1495–1499. doi:10.1126/science.1062677

Shinkura, R., K. Kitada, F. Matsuda, K. Tashiro, K. Ikuta, M. Suzuki, K. Kogishi, T. Serikawa, and T. Honjo. 1999. Alymphoplasia is caused by a point mutation in the mouse gene encoding Nf-kappa b-inducing kinase. *Nat. Genet*. 22:74–77. doi:10.1038/8780

Thompson, J.S., P. Schneider, S.L. Kalled, L. Wang, E.A. Lefevre, T.G. Cachero, F. MacKay, S.A. Bixler, M. Zafari, Z.Y. Liu, et al. 2000. BAFF binds to the tumor necrosis factor receptor–like molecule B cell maturation antigen and is important for maintaining the peripheral B cell population. *J. Exp. Med*. 192:129–135. doi:10.1084/jem.192.1.129

Thompson, J.S., S.A. Bixler, F. Qian, K. Vora, M.L. Scott, T.G. Cachero, C. Hession, P. Schneider, I.D. Sizing, C. Mullen, et al. 2001. BAFF-R, a newly identified TNF receptor that specifically interacts with BAFF. *Science*. 293:2108–2111. doi:10.1126/science.1061965

Vallabhapurapu, S., A. Matsuzawa, W. Zhang, P.H. Tseng, J.J. Keats, H. Wang, D.A. Vignali, P.L. Bergsagel, and M. Karin. 2008. Nonredundant and complementary functions of TRAF2 and TRAF3 in a ubiquitination cascade that activates NIK-dependent alternative NF-kappaB signaling. *Nat. Immunol*. 9:1364–1370. doi:10.1038/ni.1678

Weih, D.S., Z.B. Yilmaz, and F. Weih. 2001. Essential role of RelB in germinal center and marginal zone formation and proper expression of homing chemokines. *J. Immunol*. 167:1909–1919.

Willis, T.G., D.M. Jadayel, M.Q. Du, H. Peng, A.R. Perry, M. Abdul-Rauf, H. Price, L. Karran, O. Majekodunmi, I. Wlodarska, et al. 1999. Bcl10 is involved in t(1;14)(p22;q32) of MALT B cell lymphoma and mutated in multiple tumor types. *Cell*. 96:35–45. doi:10.1016/S0092-8674(00)80957-5

Wu, Y., D. Bressette, J.A. Carrell, T. Kaufman, P. Feng, K. Taylor, Y. Gan, Y.H. Cho, A.D. Garcia, E. Gollatz, et al. 2000. Tumor necrosis factor (TNF) receptor superfamily member TACI is a high affinity receptor for TNF family members APRIL and BLyS. *J. Biol. Chem*. 275:35478–35485. doi:10.1074/jbc.M005224200

Xiao, G., E.W. Harhaj, and S.C. Sun. 2001. NF-kappaB-inducing kinase regulates the processing of NF-kappaB2 p100. *Mol. Cell*. 7:401–409. doi:10.1016/S1097-2765(01)00187-3

Xue, L., S.W. Morris, C. Orihuela, E. Tuomanen, X. Cui, R. Wen, and D. Wang. 2003. Defective development and function of Bcl10-deficient follicular, marginal zone and B1 B cells. *Nat. Immunol*. 4:857–865. doi:10.1038/ni963

Yan, M., J.R. Brady, B. Chan, W.P. Lee, B. Hsu, S. Harless, M. Cancro, I.S. Grewal, and V.M. Dixit. 2001. Identification of a novel receptor for B lymphocyte stimulator that is mutated in a mouse strain with severe B cell deficiency. *Curr. Biol*. 11:1547–1552. doi:10.1016/S0960-9822(01)00481-X

Zhang, Q., R. Siebert, M. Yan, B. Hinzmann, X. Cui, L. Xue, K.M. Rakestraw, C.W. Naeve, G. Beckmann, D.D. Weisenburger, et al. 1999. Inactivating mutations and overexpression of BCL10, a caspase recruitment domain-containing gene, in MALT lymphoma with t(1;14)(p22;q32). *Nat. Genet*. 22:63–68. doi:10.1038/8767